

Smoluchowski hypernetted chain theory description of the dynamics of ions confined in charged micropores

Pedro J. Colmenares and Wilmer Olivares-Rivas

Departamento de Química, Grupo de Química Teórica, Universidad de los Andes, La Hechicera, Mérida, Venezuela

(Received 8 June 1998)

The diffusion of an ion inside a charged planar slit micropore is analyzed from a stochastic point of view. Using the instantaneous relaxation approximation (IRA), the Fokker-Planck-Smoluchowski equation was used to calculate the survival probability $G_i(x,t)$, namely, the probability that an ion of species i remains inside the pore at time t given that it started to diffuse at a given position x . The ionic density profiles were obtained using the three-point extension hypernetted chain theory (HNC), which explicitly takes into account the finite ionic sizes, and the results are compared to those using the classical modified Gouy-Chapman (MGC) theory based on the Poisson-Boltzmann point-ion equation. Calculations were carried out for a variety of pore widths, electrolyte charges, surface potentials, and absorbing or reflecting boundary conditions. We also calculate the mean first passage time (MFPT), τ , and the position-averaged MFPT, $\bar{\tau}$. Our Smoluchowski HNC results show strong discrepancies with the classical Smoluchowski MGC theory. In particular, for small pores and doubly charged coions, we observed oscillations in the position-averaged MFPT, as a function of the pore size, which are absent in the classical theory. [S1063-651X(99)09201-6]

PACS number(s): 05.20.-y, 05.40.-a, 02.50.-r

I. INTRODUCTION

The study of the dynamics of coions and counterions in electrolyte solutions, confined by charged surfaces, is of fundamental importance in the understanding of a wide variety of chemical and biophysical systems and processes. Diffusion controlled kinetics and transport phenomena in lamellar liquid crystals are just two examples [1–4].

It is common to assume that, as a central ion moves inside a charged micropore, the remaining confined ions adjust their spatial configurations instantaneously, in such a manner that the central ion moves in the one-particle equilibrium potential of mean force set up by the charged wall. Therefore, time-dependent correlation effects can be neglected. This approximation, referred to as the instantaneous relaxation approximation (IRA), was successfully used by Akesson, Chan, and others [3–5,7].

Previous studies of the ion-diffusion problem have dealt with counterions confined by two charged surfaces [3], electrolytes in a semi-infinite domain [5], or point-ion electrolytes in charged slit pores [6]. All of them are based on the IRA approximation and a Poisson-Boltzmann or Gouy-Chapman description of the nonhomogeneous ionic structure. Of particular interest is the work of Chan and McQuarrie [6], who calculated the average time for the diffusion of ions between two charged surfaces by solving the Smoluchowski equation for the one-particle propagator [1,2]. They used the ionic distribution given by the Poisson-Boltzmann equation for point ions and considered all the relevant boundary conditions for the transverse self-diffusion of ions in the charged slit.

The agreement between the MFPT obtained from Brownian dynamics and the Smoluchowski equation using the simulation potential of mean force in the IRA approximation is excellent [4,7]. However, important deviations were found when using the Poisson-Boltzmann potential of mean force,

particularly for doubly charged electrolytes.

On the other hand, it is well known that the short-range effects neglected when ions are represented by point ions are quite important when dealing with concentrated electrolyte solutions, high surface potentials, and pores of molecular dimensions.

In fact, a detailed study of the effects of the ionic size and ion-ion correlation on the equilibrium structure of electrolytes confined in charged micropores has been carried out by using the three-point extension HNC integral equation [8,9]. Different surface conditions, such as fixed zeta potential [10], fixed surface potential [11], or fixed surface charge [12,13], were analyzed for a variety of salt concentrations, charges, potentials, and pore sizes. Important quantitative and qualitative differences were found when comparing with the classical point-ion theory for the thermodynamic and electrokinetic properties. Excellent agreement was found between the HNC and the grand-canonical Monte Carlo simulations profiles, as illustrated in Fig. 1 [12–14].

In this work we study the transverse diffusion of ions of finite size within a charged slit pore of molecular dimensions. We solve the Smoluchowski equation in the IRA approximation, using the potential of mean force resulting from the solution of the HNC equation (S-HNC), and compare with the classical Smoluchowski-MGC theory (S-MGC). We obtain the survival probability and also evaluate the MFPT and the position-averaged MFPT for the boundary conditions used by Chan and McQuarrie [6] as a function of electrolyte charge and pore size.

II. THEORY

Let us model the pore as two infinite charged sheets with a given surface charge density σ_M , due to a fixed surface potential ψ_0 , on each plane and separated by a distance L . The ions are modeled as hard spheres of diameter a bearing a charge z_i on its center. As depicted in Fig. 1, the ions are

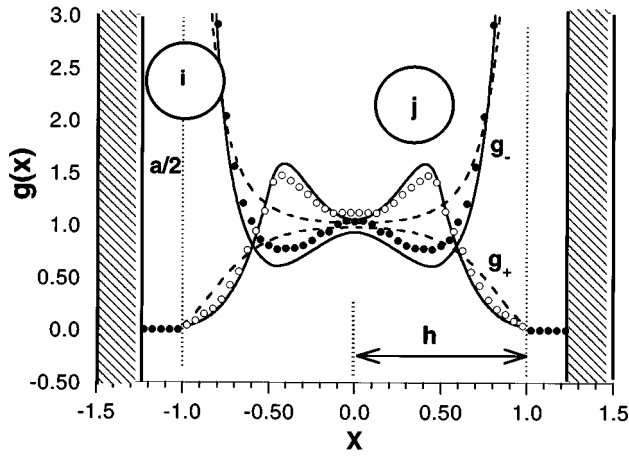


FIG. 1. Schematic representation of the planar slit pore showing the coions and counterions reduced density profiles $g_+(x)$ and $g_-(x)$ as functions of the reduced distance $x = x'/h$. Results are for a 2:2, 0.971 M RPM electrolyte in a slit formed by two walls of thickness $d = a$, separated a distance $L = 5a$, and bearing a fixed surface charge of 0.272 C/m^2 . The open and filled circles are the grand-canonical Monte Carlo data of DeGrève [14]. The continuous and dashed lines are the HNC and MGC theories, respectively.

free to move in the y and z directions but are confined to the $[-h, h]$ x domain, where $h = (L - a)/2$. The solvent is a continuous medium with a uniform dielectric constant ϵ . As we mentioned before, the objective of this paper is the application of the first passage time theory to the ions inside the pore. The theory of MFPT is well discussed elsewhere [1,2,6]. For clarity we present here a short outline of the key equations.

We approximate the instantaneous total force acting on an ion at a distance x' from the charged wall as a Langevin-like theory, i.e.,

$$\frac{dx'_i}{dt'} = v_i, \quad (2.1)$$

$$\frac{dv_i}{dt'} = -\xi v_i - \frac{dW_i(x')}{dx'_i} + \sqrt{2\xi k_B T} f_i(t'), \quad (2.2)$$

where $\xi v_i(x')$ is the hydrodynamic Markovian drag force with ξ and v_i being the friction coefficient and velocity of the ion i , respectively; $W_i(x')$ is the equilibrium potential of mean force acting on i and $f_i(t)$ is the usual δ -correlated-zero-mean white noise resulting from the collisions of the particles with ion i , i.e.,

$$\langle f_i(t') \rangle = 0, \quad (2.3)$$

$$\langle f_i(t') f_i(s') \rangle = \delta(t' - s') \quad (2.4)$$

and T and k_B are the temperature and Boltzmann constant, respectively. Though a generalized Langevin theory should be the correct formalism to describe the dynamics of the system, the lack of information about the friction kernel of the fluid confined in the charged plates obliges us to appeal to the more simplified Langevin model.

In what follows, we suppose the velocities of the ions attain a canonical distribution much faster than positions.

Thus, at the time scale of positions, velocities attain the steady state, i.e., $dv(x')/dt' = 0$ [instantaneous relaxation approximation (IRA)] so Eq. (2.1) can be written dimensionless as

$$\frac{dx_i}{dt} = \frac{d(-\beta W_i(x))}{dx} + \tilde{f}_i(t), \quad (2.5)$$

where $x = x'/h$, $t = t'D/h^2$, $h = (L - a)/2$, and $\tilde{f}_i(t) = \sqrt{2h^2/D} f_i(t)$. In the last equation, the diffusion constant D was defined by the Nernst-Einstein formula, i.e., $D = k_B T / \xi$ and $W_i(x)$ is the potential of mean force.

The potential $W_i(x')$ is crucial in our dynamical approach. Unlike previous work [6], we use results of the more physical HNC (hypernetted chain) approximation [9,11] to evaluate the potential $W(x')$ and compare it with more simplified models. Since, to our knowledge, no direct comparisons of the HNC and MGC profiles with Monte Carlo simulation data have been made for a confined electrolyte in this geometry, we present in Fig. 1 the reduced particle densities $g_i(x) = \rho_i(x)/\rho$ for coions and counterions of a 2:2, 0.971 M salt in a slit pore of width $L = 5a$, bearing a fixed charge of $\sigma = 0.272 \text{ C/m}^2$. Here the open and filled points are the coion and counterion grand-canonical Monte Carlo (GCMC) profiles of DeGrève [14]. The continuous lines are the HNC results and the dashed lines are the corresponding MGC values [12,13]. One can see from Fig. 1 that the complex structure predicted by the GCMC simulation for this system is well reproduced by the HNC theory and totally missed by the point-ions MGC approximation. In order to relate to previous work on the dynamics of ions at interfaces, in this work we will maintain conditions of fixed surface potential [11] instead of fixed surface charge [12,13]. In this case, the results are conveniently independent of the thickness of the walls [11].

Thus, from the knowledge of the density profiles for several combinations of ion charges, electrolyte concentrations, and surface potentials, we construct the potential through the expression $-\beta W_i(x') = \ln g_i(x')$, where $\beta = 1/k_B T$ and $g_i(x')$ is the normalized radial distribution function (RDF) of ions type i confined within the charged plates.

Equation (2.5) is simply the drift velocity of the ion under a stochastic potential field. Thus, if the stochastic differential equation (2.5) is interpreted in Ito's sense [2], the corresponding Fokker-Planck equation for the conditional probability $P_2 = P(x_i, t | y, t_0)$ of finding the ion in x_i at t given that it started to diffuse in y at t_0 is

$$\frac{\partial P_2}{\partial t} = -\frac{\partial}{\partial x} \left[\frac{d(-\beta W_i)}{dx} - \frac{\partial}{\partial x} \right] P_2 \quad (2.6)$$

which, as expected, is the Smoluchowski equation.

For an ion confined within the planar slit pore, the probability $G(y, t)$ of an ion to be in the diffusion domain $a < x < b$ without having been absorbed on the absorbing boundaries is simply

$$G(y, t) = \int_a^b dx_i P(x_i, t | y, t_0). \quad (2.7)$$

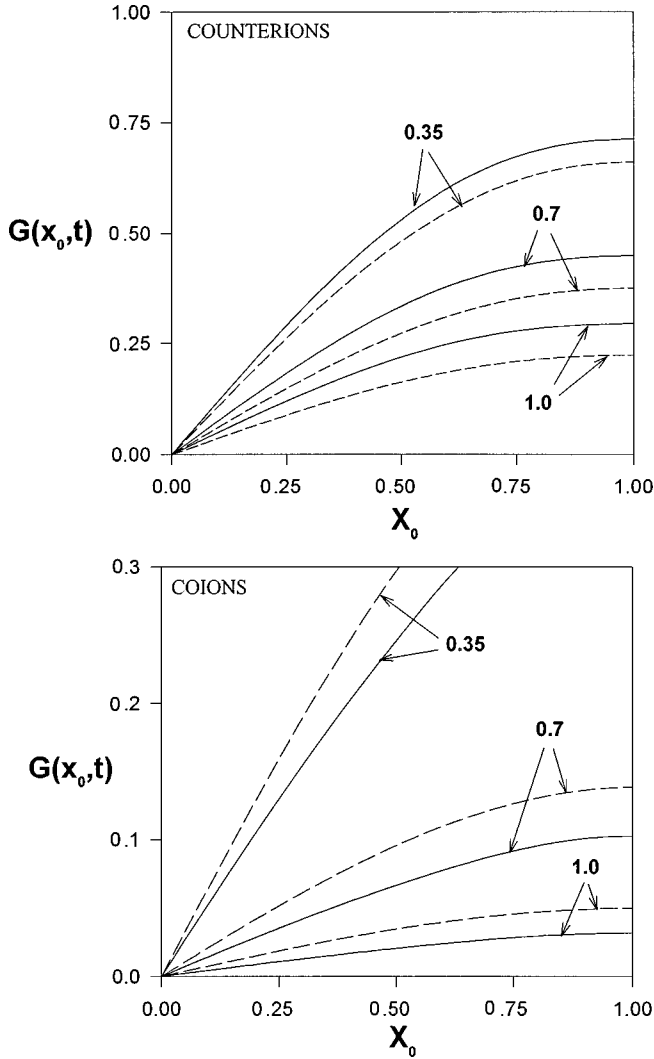


FIG. 2. A/R survival probability $G(x, t)$ as a function of the initial reduced position within the slit pore, x_0 , of counterions (upper graph) and coions (lower graph) in the domain $[0, 1]$. Results are for a 1 M, 1:1 electrolyte enclosed in a planar pore of width $L = 5a$ and a surface potential of 50 mV. The reduced times $t = Dt'/h^2$, 0.35, 0.7, and 1.0 are indicated for each curve. The dashed lines are the classical S-MGC theory while the continuous curves are our S-HNC theory. The absorbing plane is located in the center of the pore, while the plane of closest approach is reflecting.

A time evolution equation for this survival probability can be easily obtained by integrating the backward Fokker-Plank equation. The result reads [2]

$$\frac{\partial G(y, t)}{\partial t} = \frac{d(-\beta W_i(y))}{dy} \frac{\partial G(y, t)}{\partial y} + \frac{\partial^2 G(y, t)}{\partial y^2} \quad (2.8)$$

which can be solved with the initial condition $G(y, t=0) = 1$ and boundary conditions $G(y=a, t) = 0$ if the wall at a is absorbing, or $dG(y, t)/dy|_{y=a} = 0$ if it is reflecting.

Let us define $T(y)$, the first passage time (FPT), as the time needed for an ion to reach the boundary given that it started at y and $\eta(y, t)dt$ as the probability density of the $T(y)$'s. Thus for FPT's in the interval $t < T(y) < t + dt$ we find that η can be defined in terms of $G(y, t)$ as

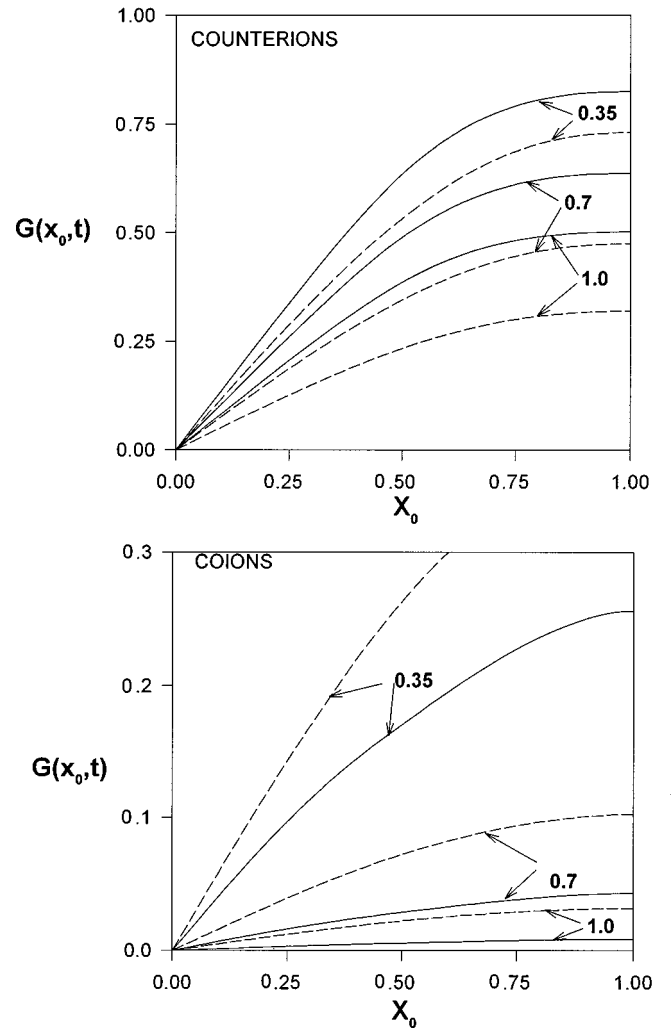


FIG. 3. A/R survival probability $G(x, t)$ as a function of the initial position within a slit pore, x_0 , of the coions (lower graph) and counterions (upper graph) for a 0.5 M, 2:2 electrolyte enclosed in a planar slit pore a width of $5a$ and surface potential of 50 mV. The notation is the same as in Fig. 2.

$$\eta(y, t) = - \frac{\partial G(y, t)}{\partial t} \quad (2.9)$$

We are particularly interested in the first moment of the distribution of FPT's, the mean first passage time (MFPT), τ , which is

$$\tau = \int_a^b dt \, t \, \eta(y, t) \quad (2.10)$$

$$= \int_a^b G(y, t) dt, \quad (2.11)$$

where the last equation is obtained after using the definition (2.9) and subsequent integration by parts. At this point, it is possible to find the ordinary differential equation which is satisfied by the $\tau(y)$'s. It is found by integrating the evolution equation for $G(y, t)$. Using Eq. (2.11) into Eq. (2.8), the result reads

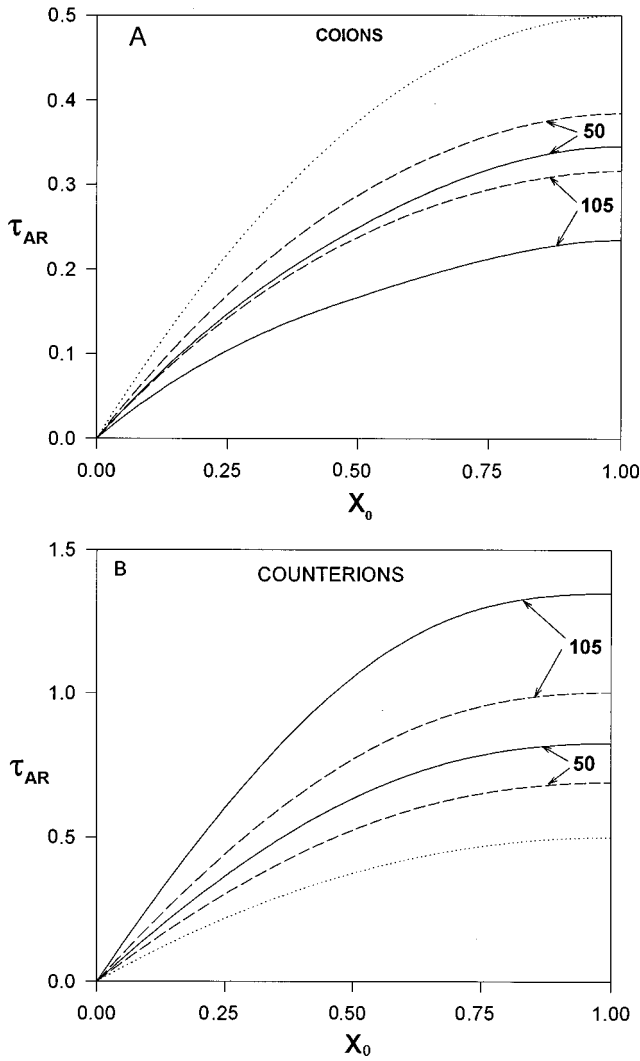


FIG. 4. A/R MFPT, τ_{AR} , as a function of the initial position x_0 for coions (a) and counterions (b) of a 1:1, 1 M electrolyte in a planar slit pore of size $5a$, and two surface potentials of 50 and 105 mV as indicated. As before, the continuous curves correspond to the S-HNC theory, the dashed curves to the S-MGC approximation, and, here as in the next figures, the dotted curve is the free-diffusion limit (FD).

$$\frac{d^2 \tau(y)}{dy^2} + \frac{d(-\beta W(y))}{dy} \frac{d\tau(y)}{dy} = -1. \quad (2.12)$$

This equation can be solved analytically. Its solution depends upon the nature of the boundary conditions, i.e., absorbing or reflecting. Thus, for a diffusion domain $[a, b]$ with $a < b$ and, noticing that $g(x) = \exp\{-\beta W(x)\}$ it is found that $\tau(y)$ is defined by

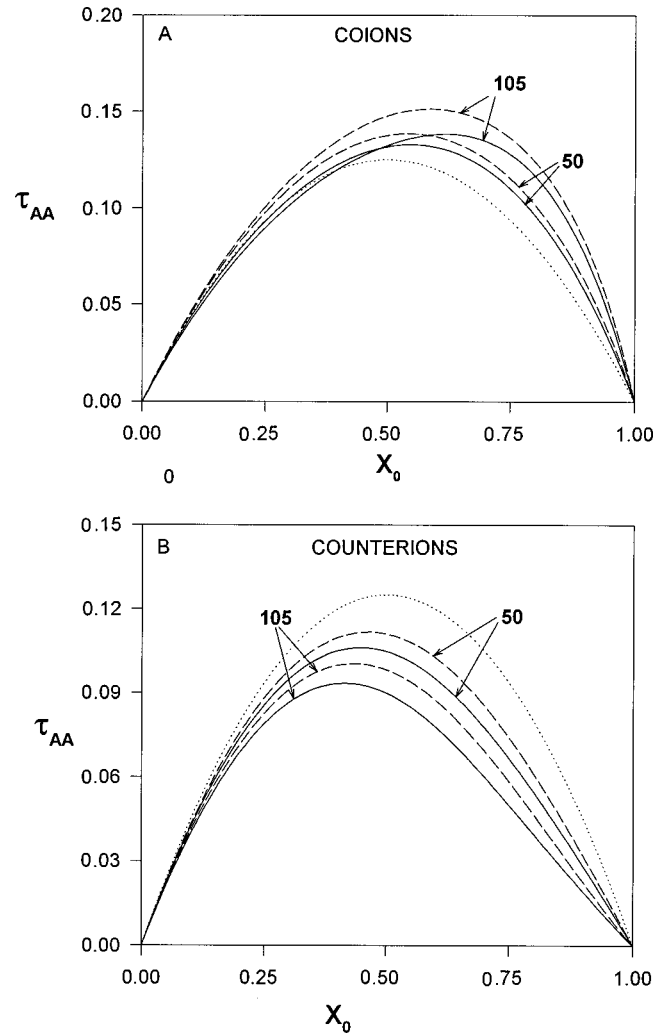


FIG. 5. A/A MFPT, τ_{AA} , as a function of the initial position, x_0 , for coions (lower graph) and counterions (upper graph) of a 1:1, 1 M electrolyte in a slit pore of size $5a$, and two surface potentials of 50 and 105 mV as indicated. Notation is the same as Figs. 1–3.

$$\tau_{AR}(y) = \int_a^y \frac{dx}{g(x)} \int_x^b g(z) dz \quad (2.13)$$

for an absorbing boundary at a and reflecting at b ,

$$\tau_{RA}(y) = \int_y^a \frac{dx}{g(x)} \int_b^x g(z) dz \quad (2.14)$$

if a is reflecting and b is absorbing, and finally, if both boundaries are absorbing

$$\tau_{AA}(y) = \frac{1}{\int_a^b \frac{dz}{g(z)}} \left[\left(\int_a^y \frac{dz}{g(z)} \right) \int_y^a \frac{dx}{g(x)} \int_b^x g(z) dz - \left(\int_y^b \frac{dz}{g(z)} \right) \int_a^y \frac{dx}{g(x)} \int_a^x g(z) dz \right]. \quad (2.15)$$

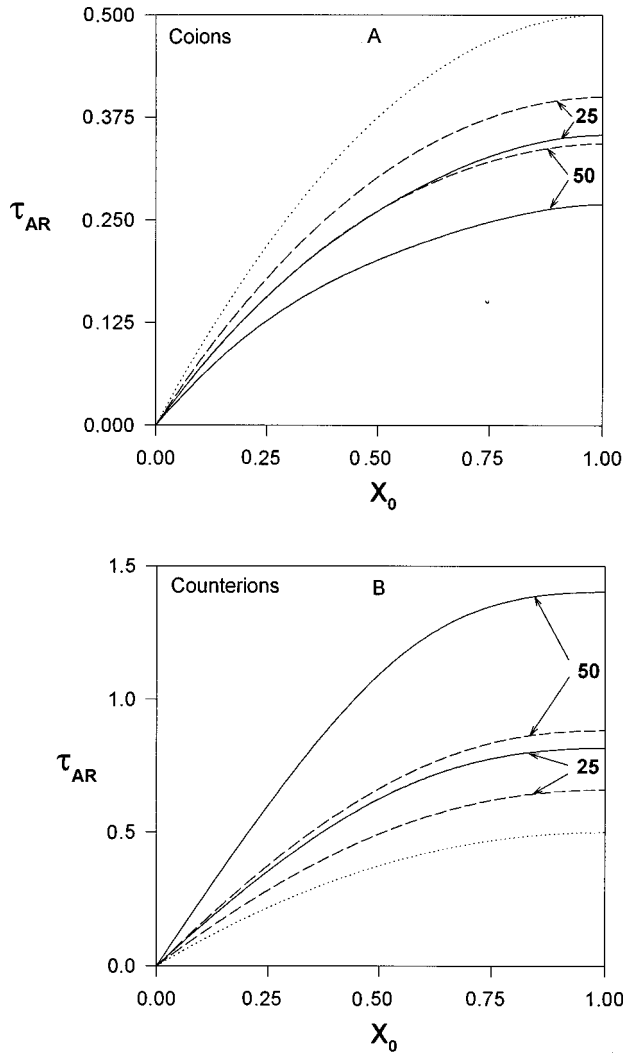


FIG. 6. A/R MFPT, τ_{AR} , as a function of the initial position for coions (lower graph) and counterions (upper graph) of a 2:2, 0.5 M electrolyte in a planar slit pore of size $5a$ and two surface potentials of 25 and 50 mV as indicated.

The position-averaged MFPT for boundaries i and j is defined as

$$\bar{\tau}_{ij} = \int_a^b \tau_{ij}(y)g(y)dy. \quad (2.16)$$

Equations (2.8) and (2.13)–(2.16) are the central results needed in this paper.

III. RESULTS AND DISCUSSION

We have solved numerically both the S-HNC and S-MGC differential equations for model 1:1 and 2:2 electrolytes confined to a slit pore at constant surface potential. The equilibrium radial distribution functions obtained from the numerical solution of the integral equations [11] were accurately fitted using a spline algorithm, to allow easy handling of the data.

Figure 2 shows the survival probability $G(x,t)$ as a function of the initial position x_0 for a 1:1, 1 M RPM electrolyte in a planar slit pore of width $L = 5a$, having a surface poten-

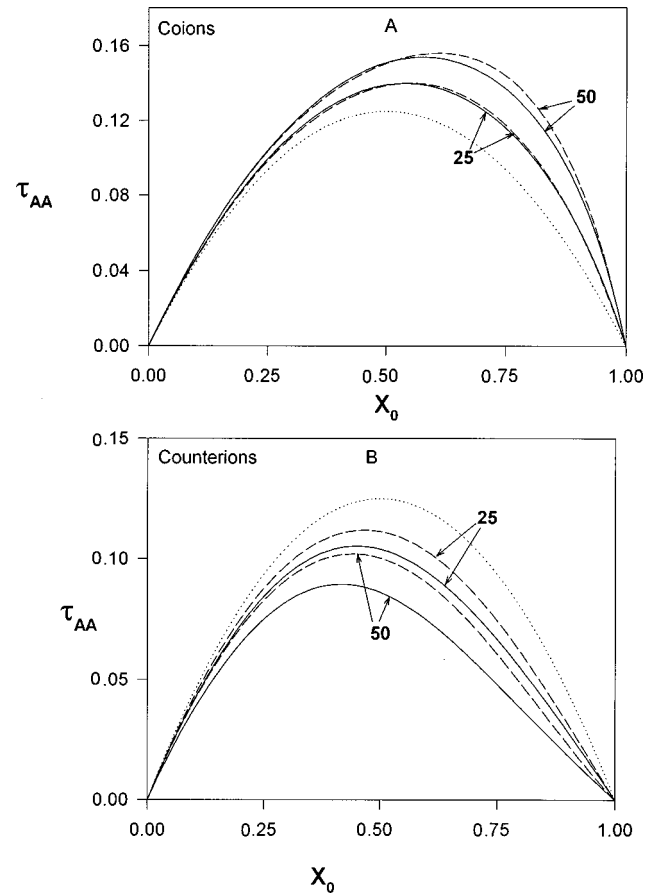


FIG. 7. A/A MFPT, τ_{AA} , as a function of the initial position, x_0 , for coions (lower graph) and counterions (upper graph) of a 2:2, 0.5 M electrolyte in a pore of size $5a$ and two surface potentials of 25 and 50 mV as indicated.

tial $\psi = 50$ mV. The diffusion domain corresponds to an A/R boundary condition where the absorbing plane is located at the middle of the slit pore $x = 0$ and the reflecting planes are located at the planes of closest approach at $x = -1$ and 1 . Results are for several reduced times $t = Dt'/h^2$ as indicated for each curve. The continuous curves are our S-HNC result and the dashed curves are the S-MGC classical theory. The upper graph, Fig. 2(a), corresponds to the counterions and the lower graph, Fig. 2(b), to the coions.

Here $G_j(x_0, t)$ measures the probability that at time t an ion of type j , originally located at x_0 , has not yet been absorbed by the midplane to the left. Then $G(x_0, t) \rightarrow 0$ as $x_0 \rightarrow 0$ and $G(1, 0) = 1$. Though not shown, for very small times the survival probability for counterions and coions are very similar. However, as the time evolves a difference in the dynamics of counterions and coions develops, as shown in Fig. 2. Since the coions are repelled by the walls, their survival probability becomes lower than that of the counterions. The effect of the ionic size and ion-ion correlations cause an increase in $G_j(x_0, t)$ for the counterions and, correspondingly, a decrease for the coions. This is illustrated by the differences between the S-HNC and S-MGC curves. That is, the finite-size counterions are allowed to remain away longer from the absorbing midplane, while the finite-size coions are further pushed towards the midplane. These differences are

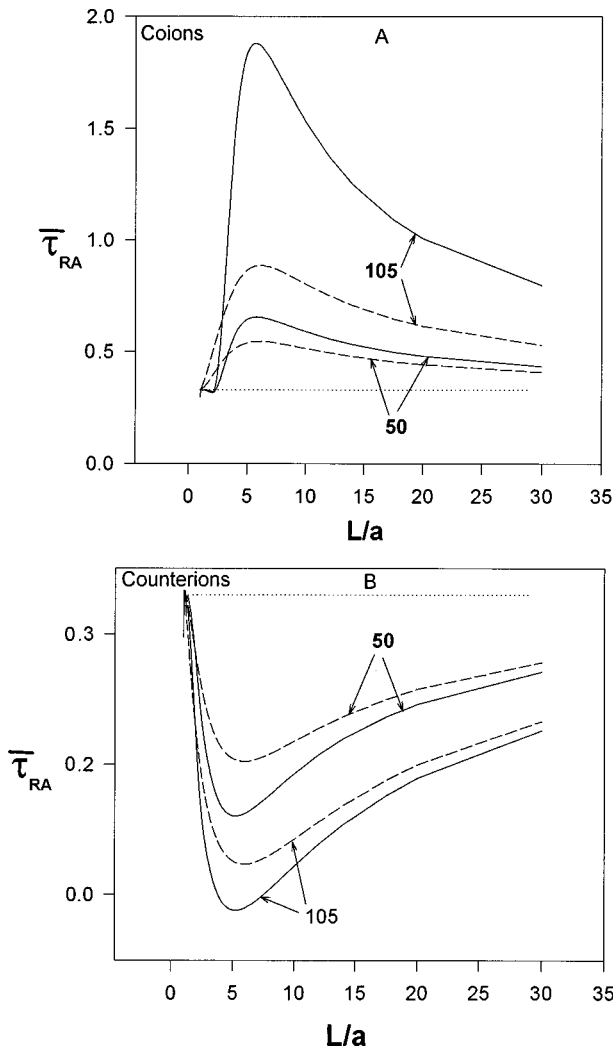


FIG. 8. Reduced position-averaged MFPT, $\bar{\tau}_{RA}$, as a function of the pore size parameter L/a for R/A conditions in $[0,1]$ or A/A in $[-1,1]$ for coions (lower graph) and counterions (upper graph) for a 1:1, 1 M electrolyte and two surface potentials of 50 and 105 mV as indicated. The free-diffusion limit corresponds to the value $\frac{1}{3}$.

larger the closer the ions are from the reflecting walls at the beginning.

The behavior of the survival probability for a doubly charged 2:2, 0.5 M electrolyte solution is shown in Fig. 3. Results are for the same reduced times and conditions as Fig. 2, keeping the potential at 50 mV. Here, we clearly see a marked increase both in differences between the survival of counterions and coions in the slit pore and in the discrepancies between the S-HNC and the S-MGC theories. The survival probability of the coions decreases as the ionic charge is increased. This difference is more notorious in the S-HNC approach, which considers more rigorously the ion-ion short-range correlations. We observe in Figs. 2 and 3 that, in general, the S-MGC classical theory overestimates the survival of the coions and underestimates the survival of the counterions.

Figure 4 shows the mean first passage time, $\tau_{AR}(x_0)$, for absorbing/reflecting boundary conditions (A/R) as a function of the initial reduced position x_0 for coions (a) and counterions (b) of 1:1, 1 M electrolyte in a planar slit pore of size $5a$, and two surface potentials of 50 and 105 mV as

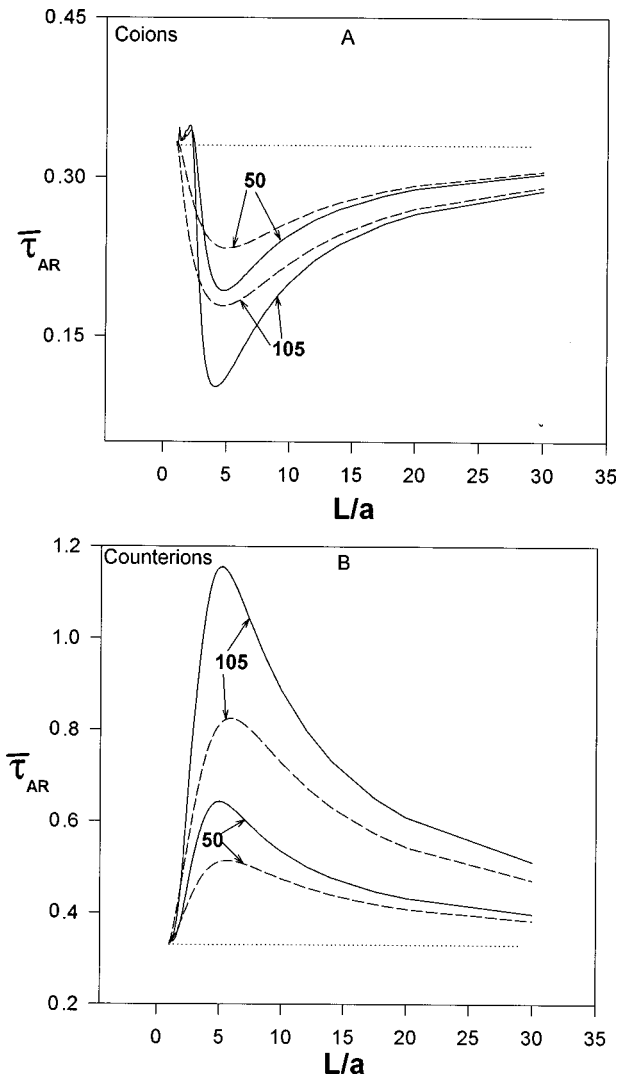


FIG. 9. Reduced position-averaged MFPT, $\bar{\tau}_{AR}$, as a function of the pore size parameter L/a for A/R conditions in $[0,1]$ for coions (lower graph) and counterions (upper graph) for a 1:1, 1 M electrolyte and two surface potentials of 50 and 105 mV as indicated. The free-diffusion limit corresponds to the value $\frac{1}{3}$.

indicated. The continuous curves correspond to the S-HNC theory, the dashed curves to the MGC approximation, and the dotted curve is the free-diffusion limit (FD). As expected, the MFPT goes to zero as the initial position of the diffusing particle gets closer to the absorbing boundary. Due to the electrical field, coions are pushed away from the reflecting surface at $x=1$ in the direction of the absorbing plane at $x=0$, giving rise to MFPT's that are lower than those expected in the free-diffusion limit. The opposite occurs to the counterions. The ion-ion correlations due to the finite ion size have the effect of lowering the MFPT of the coions and increasing it for the counterions. This can be seen by comparing the S-HNC results to those of the S-MGC since the latter neglects those correlations. Both the effect of the electrostatic potential and the interionic correlations increase with the surface potential.

Figure 5 shows the MFPT as a function of the initial reduced position x_0 for coions (a) and counterions (b) for the same system as Fig. 4 but for an absorbing/absorbing (A/A) boundary condition. Here we have three absorbing bound-

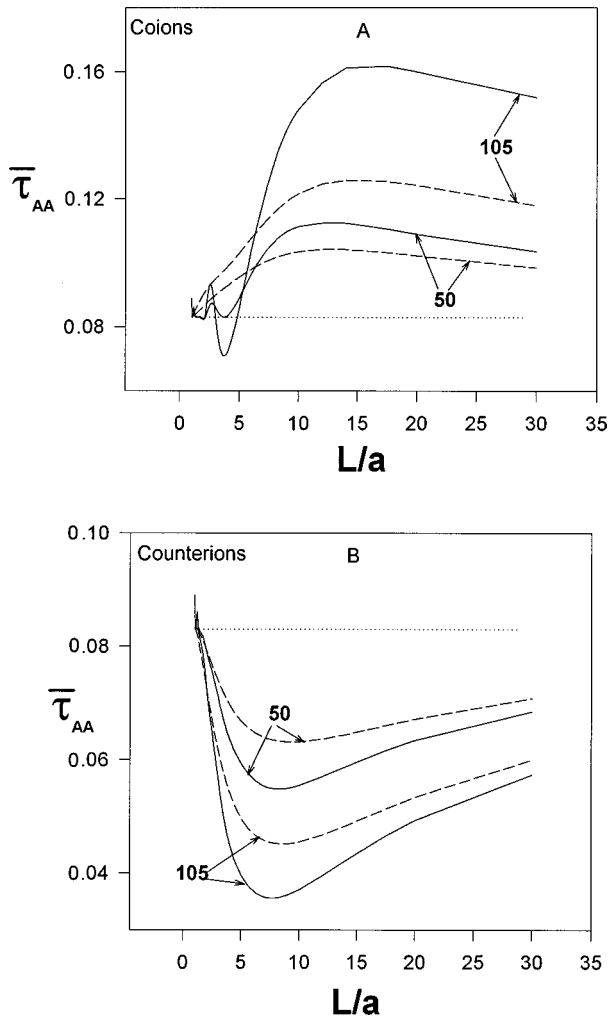


FIG. 10. Reduced position-averaged MFPT, $\bar{\tau}_{AA}$, as a function of the slit pore size parameter L/a for A/A conditions in $[0,1]$ for coions (lower graph) and counterions (upper graph) for a 1:1, 1 M electrolyte and two surface potentials of 50 and 105 mV as indicated. The free-diffusion limit corresponds to the value $\frac{1}{12}$.

aries, one at the midplane of the slit pore and the others at the plane of closest approach. The MFPT in the free-diffusion limit is symmetric with respect to the two absorbing planes, around $x=0.5$. In the MGC approach, the effect of electrostatic ion-surface interaction causes an asymmetry. The MFPT curves are shifted to the right-hand side for the coions, giving larger times, and to the left-hand side for the counterions, giving lower times. A similar situation occurs in the HNC approach, but here the asymmetric behavior is more complex, particularly for the coions, as the potential is increased. In general, the interionic correlation, neglected in the MGC approach, favors the absorption of the coions and delays the absorption of the counterions. Again, all the observed effects are enhanced by a larger surface potential.

Figures 6 and 7 show the A/R and A/A MFPT's as functions of the initial position for coions (a) and counterions (b) of a 2:2, 0.5 M electrolyte in a planar slit of size $5a$, and two surface potentials of 25 and 50 mV as indicated. These figures show the effect of the ionic charge on the MFPT for A/R and A/A boundary conditions. In general, the separation from the free-diffusion limit and the discrepancy between the S-HNC and S-MGC theories is increased as the ionic charges

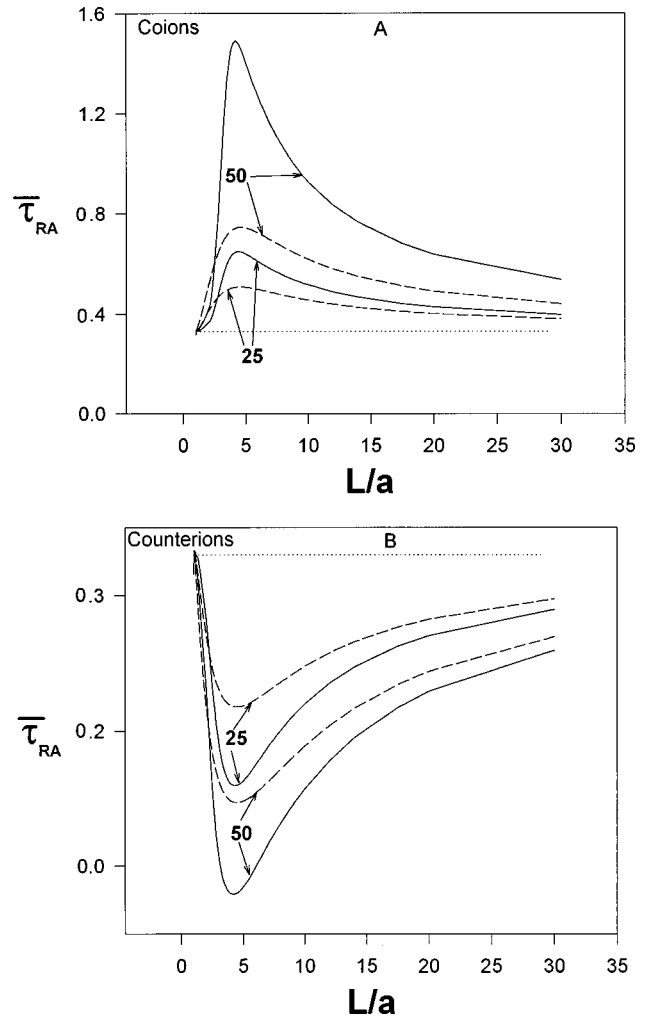


FIG. 11. Reduced position-averaged MFPT, $\bar{\tau}_{RA}$, as a function of the pore size parameter L/a for R/A conditions in $[0,1]$ or A/A in $[-1,1]$ for coions (lower graph) and counterions (upper graph) for a 2:2, 0.5 M electrolyte and potentials of 25 and 50 mV as indicated. The free-diffusion limit corresponds to the value $\frac{1}{3}$.

increase. Namely, in an absorbing/reflecting situation the doubly charged coions are absorbed faster, while the doubly charged counterions are absorbed at larger times, as compared to the singly charged ions under similar conditions.

The position-averaged mean first passage time $\bar{\tau}$ corresponds to the mean time that a given species takes to be absorbed irrespective of its initial position in the diffusion domain. For R/A and A/R conditions in the domain $[0,1]$, free diffusion gives $\bar{\tau} = \frac{1}{3}$.

In Figs. 8–10, we show the effect of the slit pore size on the reduced position-averaged MFPT, $\bar{\tau}$, for three different absorption conditions. Figure 8 shows the reduced position-averaged MFPT as a function of the pore size parameter, L/a , for R/A conditions in the domain $[0,1]$ or A/A in $[-1,1]$ for coions (a) and counterions (b) for a 1:1, 1 M electrolyte, and two surface potentials of 50 and 105 mV as indicated. The free-diffusion limit corresponds to the value $\frac{1}{3}$. Figure 9 corresponds to A/R conditions in $[0,1]$ for which the free-diffusion limit also corresponds to the value $\frac{1}{3}$. Figure 10 shows the results for A/A conditions in $[0,1]$. Here, the free-diffusion limit corresponds to the value $\frac{1}{12}$.

For R/A conditions the absorbing plane is located at the

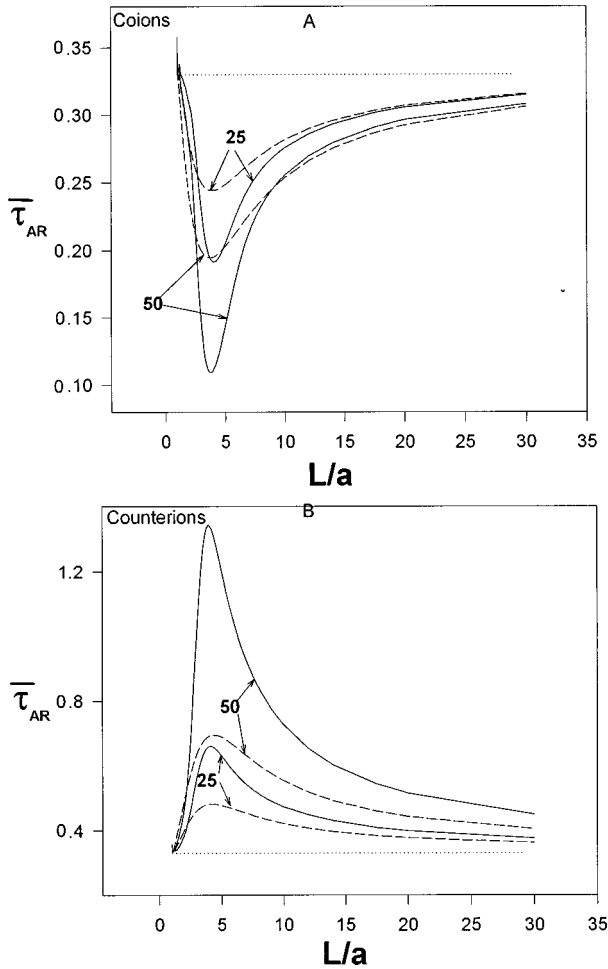


FIG. 12. Reduced position-averaged MFPT, $\bar{\tau}_{AR}$, as a function of the pore width, L/a , for A/R conditions in $[0,1]$ for coions (lower graph) and counterions (upper graph) for a 2:2, 0.5 M electrolyte and surface potentials of 25 and 50 mV as indicated. The free-diffusion limit corresponds to the value $\frac{1}{3}$.

plane of closest approach to the surface and, therefore, deviations from the free-diffusion limit, the value $\frac{1}{3}$ in this case, are higher for the coions and lower for the counterions, as shown in Fig. 8. The ion-ion short-range correlations due to the finite ionic sizes have the effect of further increasing the coion position-averaged MFPT while decreasing that of the counterions, as shown by the strong discrepancies between the S-HNC and S-MGC theories in Fig. 8. The absorption time shows a maximum for the coion and a minimum for the counterions for pores of sizes close to $5a$. When the absorbing plane is located at the midplane of the planar slit pore, under A/R conditions, the situation is reversed for coions and counterions, as shown in Fig. 9.

When both the midplane and the plane of closest approach are absorbing (A/A), the maxima and minima are shifted to larger pore sizes, as shown in Fig. 10. Additionally, while the counterions present deviations from the free-diffusion limit similar to those observed in the R/A condition, the coions present an oscillatory behavior when described by our S-HNC theory. This effect is not predicted by the S-MGC theory. In fact, these oscillations seem to have the same origin in the short-range interactions as does the net force between the plates, as observed both experi-

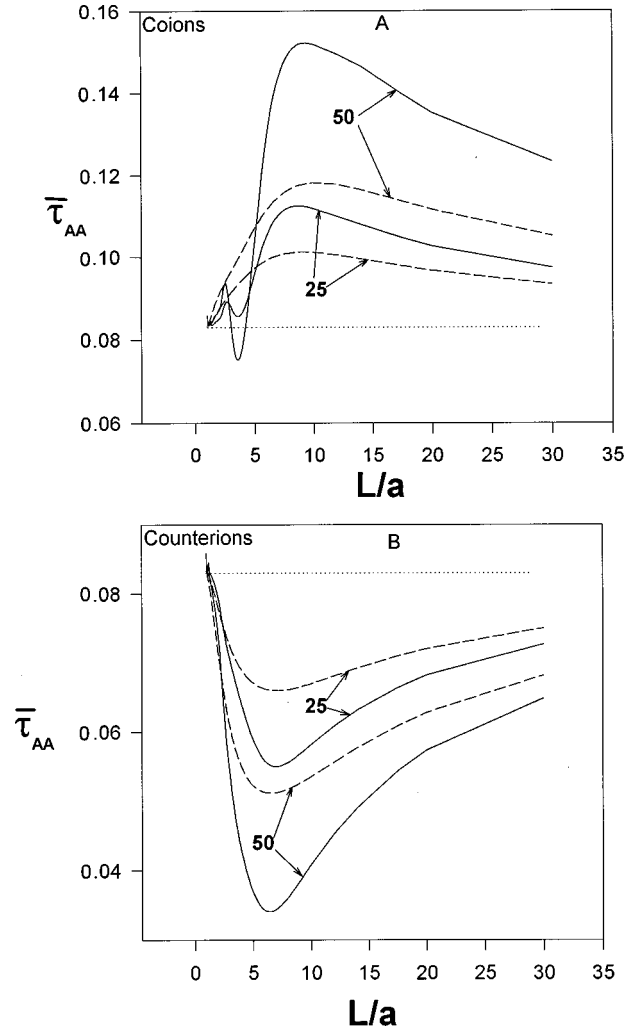


FIG. 13. Reduced position-averaged MFPT, $\bar{\tau}_{AA}$, as a function of the pore width, L/a , for A/A conditions in $[0,1]$ for coions (lower graph) and counterions (upper graph) for a 2:2, 0.5 M electrolyte and surface potentials of 25 and 50 mV as indicated. The continuous curves correspond to our S-HNC results, the dashed curves to the S-MGC approximation, and the free-diffusion limit (dotted line) corresponds to the value $\frac{1}{12}$.

mentally and theoretically [11,15]. Namely, they are due to the hard-sphere short-range interactions. The irregular small oscillations observed for very narrow slit pores, close to $L = a$, are just a feature of the numerical integration, since very few points were used.

Figures 11–13 show that the effects described in Figs. 8–10 for 1:1 electrolytes are strongly enhanced for a doubly charged 2:2 electrolyte. The short-range ion-ion and ion-interface correlations are originated in our model by the fact that ions have a finite diameter a . However, such correlations are coupled with the long-range electrostatic interactions, due to the wall's electrical field and the Coulomb ion-ion potential. As a consequence, an increase on the ionic charge or on the surface potential has the effect of magnifying the importance of the short-range correlations, particularly for slit pores a few ionic diameters wide.

IV. CONCLUSIONS

We have described the dynamics of ions inside narrow charged slit pores in terms of the survival probability

$G_i(x, t)$, the mean first passage time $\tau(x)$, and the position-averaged MFPT, $\bar{\tau}$, for a variety of absorbing and reflecting boundary conditions.

The numerical solution of the Smoluchowski equation together with the HNC equilibrium profiles, under the instantaneous relaxation approximation (IRA), allowed the explicit consideration of the ion-ion short-range correlations and ionic size effects. These effects had been previously neglected in the classical theory based on the Poisson-Boltzmann approximation [6]. As expected, the dynamics of both coions and counterions is strongly modified by these effects, as can be seen by comparing our S-HNC results with the corresponding S-MGC.

In general, the electrostatic surface-ion interaction has the effect of increasing the time that a coion spends inside a slit pore before it is absorbed, $\bar{\tau}_{AA}$, as compared to the situation of a noninteracting free-diffusing particle. However, the oscillations observed on $\bar{\tau}_{AA}$ indicate that a doubly charged

coion could spend less time than a free-diffusing particle for certain sizes of the micropore. This effect seems to have its origin in the continuous spatial rearrangement of the ions due to the interplay of short-range and electrostatic ion-ion and ion-charged wall correlations absent in the S-MGC theory. These findings could have particular relevance for the chemistry of confined ionic systems.

ACKNOWLEDGMENTS

This work was financed by CONICIT, Venezuela through Grant No. S1-2503. It was finished while W.O.R. was on sabbatical leave at Universidad Autónoma de México. W.O.R. acknowledges CONACYT for the Cátedra Patrimonial de Excelencia granted. We thank B. Sulbarán for the valuable discussions about the equilibrium data, and L. DeGrève for providing the GCMC data prior to publication.

-
- [1] G. H. Weiss, *Adv. Chem. Phys.* **13**, 1 (1967).
 [2] C. W. Gardiner, *Handbook of Stochastic Methods for Physics, Chemistry and the Natural Sciences* (Springer-Verlag, Berlin, 1985).
 [3] D. Y. Chan and B. Halle, *Biophys. J.* **46**, 387 (1984).
 [4] T. Åkesson and B. Jönsson, *J. Phys. Chem.* **89**, 2401 (1985).
 [5] D. Chan, *J. Chem. Soc., Faraday Trans. 2* **83**, 2271 (1987).
 [6] D. Chan and D. McQuarrie, *J. Chem. Soc., Faraday Trans. 2* **86**, 3585 (1990).
 [7] B. Jönsson and H. Wenneström, in *Micellar Solutions and Microemulsions*, edited by S. H. Chen and R. Rajagopalan (Springer-Verlag, New York, 1990).
 [8] M. Lozada-Cassou and E. Díaz-Herrera, *J. Chem. Phys.* **92**, 1194 (1990).
 [9] M. Lozada-Cassou and E. Díaz-Herrera, *J. Chem. Phys.* **93**, 1386 (1990).
 [10] E. González-Tovar, M. Lozada-Cassou, and W. Olivares, *J. Chem. Phys.* **94**, 2219 (1991).
 [11] W. Olivares, B. Sulbarán, and M. Lozada-Cassou, *J. Chem. Phys.* **103**, 8179 (1995).
 [12] M. Lozada-Cassou, W. Olivares, and B. Sulbarán, *Phys. Rev. E* **53**, 522 (1996).
 [13] B. Sulbarán, M.Sc. thesis, Universidad de Los Andes, Venezuela, 1992.
 [14] L. DeGrève (unpublished).
 [15] J. N. Israelchvili and G. E. Adams, *J. Chem. Soc., Faraday Trans. 1* **74**, 975 (1978).